Magnetic Charts in Antarctica and Neighboring Areas

LEROY R. ALLDREDGE and ZURAB KOBIASHVILI

Institute for Earth Sciences, Environmental Science Services Administration, Boulder, Colorado, U. S. A.

Abstract: Data, from many available recent sources, on the magnetic field in Antarctica and neighboring areas are intercompared. Field values were computed for the spherical harmonic models of HURWITZ *et al.*, and LEATON *et al.*, for 1965 at intervals of 5° in latitude and 10° in longitude between 40°S and the South Pole. The rms differences were 0.76° for *D*, 0.43° for *I* and 185 gammas for *H*. A similar comparison between the model of CAIN for 1960 and the model of NAGATA and OGUTI for 1958.5 updated to 1960 gave rms differences of 3.0°, 0.93° and 775 gammas for *D*, *I*, and *H* respectively. Comparison between the 1965 models and several recent traverses indicate that the LEATON model is more accurate in this area than the HURWITZ model. Comparison between earlier traverses and the 1960 models favor the CAIN model over the NAGATA and OGUTI model, although part of this may be caused by uncertain secular change data used to bring the model up to the date of the traverses.

Introduction

Due to its inaccessibility, the data net covering Antarctica and neighboring areas has naturally been quite sparse as compared to many other regions of the earth. Historically, the first magnetic survey in this general region of the earth was HALLEY's voyage in the PARAMOUR PINK in 1698–1700 which went as far south as the 52° parallel. In 1701, HALLEY utilized his observations and compiled the first oceanic magnetic declination chart. A year later, using observations made by other mariners, he compiled the first world magnetic chart.

A means of providing a synoptic picture of the world distribution of the magnetic field and its secular change was developed by GAUSS in 1832 when he provided a method of measuring the magnetic intensity in absolute units. Two years later, he set up the first magnetic observatory at Göttingen at which all three magnetic elements could be measured. With the assistance of HUMBOLT, GAUSS succeeded in arousing scientific interest; the ensuing program was one of the first examples in international cooperation in the study of a world wide phenomena. Observatories were established and surveys undertaken encompassing regions where no previous observations had ever been made. The best known outgrowth of this period was the expedition of Ross in 1840–41 to the vicinity of the South Magnetic Pole (CHAPMAN, 1964; NELSON, HURWITZ and KNAPP, 1962).

Even as late as the first quarter of the twentieth century, information regarding the compass direction in polar regions was almost completely based on

theories developed by GAUSS and LAMONT in the first part of the nineteenth century (FLEMING, 1939). An Index Chart of Antarctic Magnetic Observations compiled by D. G. KNAPP of the U. S. Coast and Geodetic Survey shows that as late as 1946 the major portion of magnetic observations in the Antarctic region and neighboring areas lay between the 50° and 60° parallels and along the coast of the Ross Ice Shelf and Victoria Land. The lack of data in this portion of the world resulted in magnetic observations in other areas determining the chart values of the magnetic field in Antarctica.

In the last decade and a half, the situation has considerably improved. Magnetic surveys in the Antarctic region are being carried on by the U. S. Navy's Project Magnet. Satelliteborne magnetometers are providing us with knowledge of the spatial distribution of the magnetic field over the polar regions as well as the rest of the earth. During the IGY, geomagnetic measurements were undertaken in Antarctica which contributed to the compilation of the British Admiralty World Magnetic Charts and the U. S. Hydrographic Office World Magnetic Charts both for 1960. During the International Quiet Sun Year (IQSY), magnetic surveys were made on land, at sea and by aircraft, satellites and rockets. Also, since 1957, the U. S. Coast and Geodetic Survey in cooperation with various universities has run magnetic traverses in Antarctica. Other nations such as the U.S.S.R., Japan, France, Belgium and England have also conducted Antarctic expeditions for the purpose of obtaining geomagnetic and geophysical data.

Methods of Reduction

Four models considered to be representative were intercompared. They are the models of LEATON, MALIN and EVANS (1965), henceforth referred to as the LME model; and the model of HURWITZ, KNAPP, NELSON and WATSON (1966) referred to as the HKNW model, both for epoch 1965. The models for epoch 1960 are the Goddard Space Flight Center model of CAIN (1965) and the model of NAGATA and OGUTI (1962), to be referred to as the N & O model, for 1958.5 updated to 1960.

Besides some variation in the method of spherical harmonic analysis, the major differences between the models is in the methods of data reduction. The methods of smoothing and the criteria used for the acceptance of values varied appreciably from model to model.

In the LME reduction, the secular change for D (1960) and H & Z (1955) were used in producing corrected working manuscript World Charts for D (1960) and H & Z (1955) by reducing to the proper epoch all recent observations available by mid-June 1964. Also where reliable local survey charts existed, they were brought up to epoch and superimposed on the working charts. An averaging method was used on the Project Magnet data and a linear interpolation-reduction method was used on the 2500 observations of the magnetic declination made by merchant ships since 1961. Where it was considered that the elements were sufficiently well known, values of D, H, and Z were obtained from these

corrected charts for use in the harmonic analysis. Between 60°S and 60°N, the grid separation was 10° in longitude and latitude. For 70° and 80° N and S the separation was 20° in longitude but in a staggered fashion between the two parallels. H and Z were brought up to 1965 by means of the secular change for 1960; the secular change for 1962.5 was utilized for D. (This secular change chart was deduced from graphical modifications of the 1960 values to fit the annual change at permanent observatories.) Preliminary spherical harmonic analyses to the 6th and 8th order were performed on this corrected updated data. The 8th order solution gave a better fit to observed data. Three further analyses to degree and order 8 were performed; for these analyses, observed values were included where they were thought to be more accurate that the values derived from the previous analyses.

A combination computerized and graphical method was used in the reduction to 1965 of the 425,000 magnetic measurements made since 1900 which were available for the HKNW analysis. A value of Z reduced to 1965 was obtained at every station where reduced values of I and H were available. These reduced values were averaged over one-degree quadrangles. During this process, values of D and H having residuals greater than 2° or 1000 gammas were usually discarded as were values of Z that depended on measurements made before 1930. This was done because of the increased use of earth inductors after that date. A quadratic polynomial smoothing and interpolating method was applied to the resulting 20,000 partially edited one degree quadrangular means in overlapping 30° by 30° grid areas with 10° between centers. In areas where D and H developed singularities, such as in the polar regions, a method developed by KNAPP (1966) was used in obtaining the grid values for D and H from which X and Y were then computed. At this point, incomplete sets of 5° grid values for X, Y and Z were available; 10° subsets of these (still incomplete) were used as input to a preliminary spherical harmonic analysis to degree and order 9. A complete set was then obtained and used as input to an analysis to degree and order 12.

The CAIN analysis for 1960 utilized data ranging from 1945 to 1964 and included data from satellites (Vanguard III and Alouette). Only a small amount of data deletion was done; surface and aircraft data were only "clipped" in areas of 2° by 2° in longitude and latitude where the density exceeded 100 observations per 10^5 km^2. Also observatory data was weighted by a factor of 2 to 4 times that of the other survey data.

NAGATA and OGUTI reduced the newly obtained Antarctic data to 1958.5 by means of the isoporic charts for 1955–60. Because of the lack of a high density of observational points in Antarctica, the condition that $\partial X/\partial y = \partial Y/\partial x$ which follows from the requirement that curl F be zero, was required in the drawing of the isodynamic charts for X and Y. These values were compared to the British Admiralty Charts for 1955 reduced to 1958.5; the Admiralty Charts were then corrected by the new Antarctic data south of the 55°S latitude circle. The X, Y and Z values so obtained were then subjected to a spherical harmonic

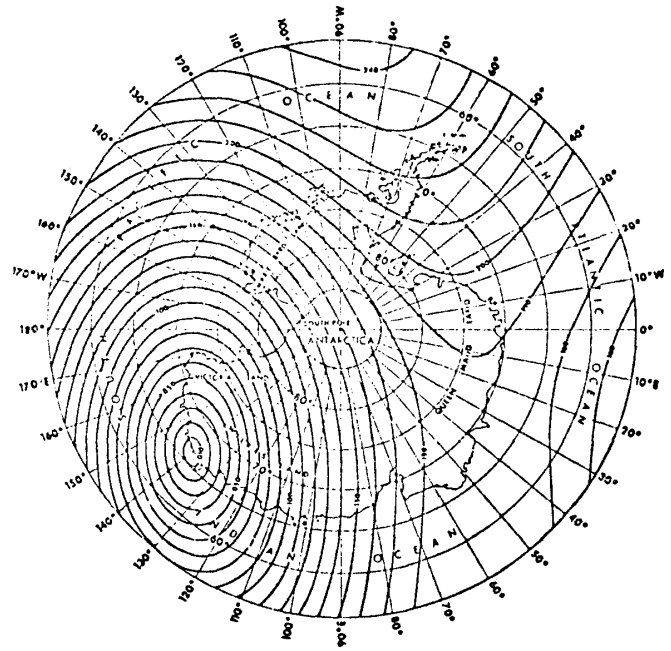

Fig. 1(a). The horizontal intensity component for the earth's magnetic force for epoch 1965, derived from the model of HKNW.

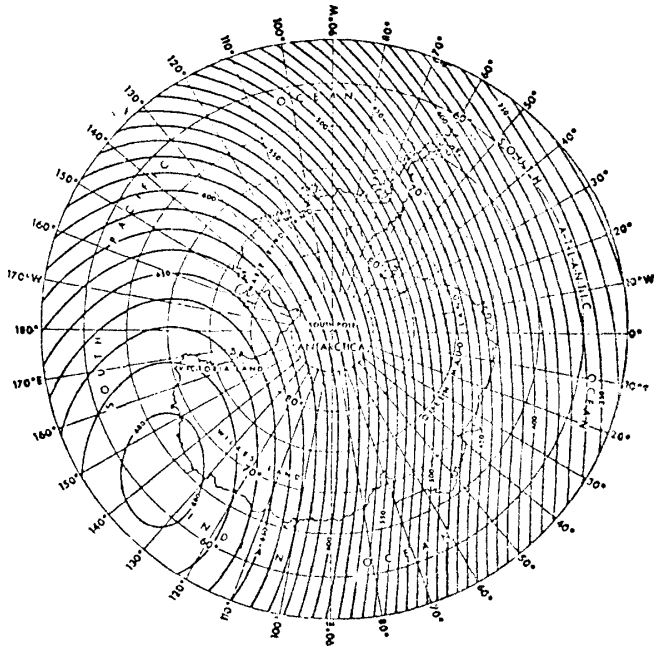

Fig. 1(b). The total intensity of the earth's magnetic force for epoch 1965, derived from the model of HKNW.

analysis to degree and order 6.

The Spherical Harmonic Analysis

The general expansion for the geomagnetic potential with coefficients of internal and external origin is of the form (CHAPMAN and BARTELS, 1940, p. 639)

$$V=a\sum_{n=1}^{\infty}\left((r/a)^n T_n^e+(a/r)^{n+1} T_n^i\right)=V^e+V^i \qquad (1)$$

where

$$T_n=\sum_{m=0}^{n}(g_n^m\cos m\lambda+h_n^m\sin m\lambda)\,P_n^m(\theta) \qquad (2)$$

where the i and e superscripts refer to the internal and external sources and a, θ and λ refer to the earth's radius, colatitude and longitude with the p_n^m's being the LEGENDRE associated function in the SCHMIDT quasi-normalized form.

In the LME, N&O and HKNW analyses, the X and Y components were coupled; that is the observational equations from both components contributed to the same set of normal equations. In the LME analysis, the external contribution to the potential was assumed to be zero. Since the external coefficients are always less than 100 gammas in magnitude, they are frequently ignored in comparison to the internal coefficients (LEATON, 1957; NAGATA and OGUTI, 1962). Figure 1 shows two of the U. S. 1965 Magnetic Charts for the Antarctic and neighboring areas which were produced from the HKNW analysis.

The CAIN analysis for 1960 assumed a spheroidal instead of a spherical earth. This is done by using the geocentric radius and geocentric colatitude, ϕ, in the normal equations instead of the geodetic colatitude θ and a radius derived from the mean earth's radius. In order to be consistent with the direction of measured data, a further correction is made for the angular difference between the geocentric and geodetic latitude. If F_r, F_ϕ, and F_λ are the geocentric components of $F=-\nabla V$ and if d is the angle of rotation between the geocentric and geodetic latitude (about 0.2°), then the measured X, Y and Z components of the field are given by (CAIN *et al.*, 1965)

$$X=-F_\phi\cos d-F_r\sin d$$
$$Y=F_\lambda$$
$$Z=F_\phi\sin d-F_r\cos d,$$

where $\sin d=\sin\alpha\sin\phi-\cos\alpha\cos\phi$ and α is the geodetic latitude.

The CAIN external field contained only the first three spherical harmonic coefficients. This had the effect of applying a uniform flux of less than 30 gamma across the earth.

Points of Singularity

The horizontal magnetic field component, the inclination and declination all have points of singularity at the magnetic dip poles. The region around the dip poles exhibit sharp curvature in these isolines and they tend to become elongated especially in the Arctic.

These peculiar characteristics make it very difficult to smooth sketchy data in the dip pole areas. For this reason unusual techniques, which involve a transformation of the coordinate system and use of different magnetic components, have been used to simplify the problem.

Consider a region around the dip pole sufficiently small so that it can be approximated as a plane. The relationships between rectangular distances x and y and polar coordinates β and ρ with the origin on the dip pole are $x=\rho\cos\beta$ and $y=\rho\sin\beta$. If the x and y directions coincide with the principal axis of the magnetic potential the lines of equipotential described in CHAPMAN (1940) have the form (CHAPMAN, 1941)

$$V=V_0+\frac{1}{2}(ax^2+by^2) \tag{4}$$

where V_0 is the value of the potential at the pole. The H-isodynamic lines have the form

$$H^2=(-\partial V/\partial x)^2=a^2x^2+b^2y^2 \tag{5}$$

$$H=\rho(a^2\cos^2\beta+b^2\sin^2\beta)^{\frac{1}{2}}$$

Equation (5) has the form of a family of ellipses of eccentricity $(1-a^2/b^2)^{\frac{1}{2}}$. Since the term H/ρ is only a function of β, the contour lines form an elliptical cone which has no unique gradient at the dip pole. As r approaches 0, the derivative remains finite and non-zero, hence the function H is not a regular function in this area since its gradient is not continuous at the dip pole. Since $H=0$ at the pole, and since H is an otherwise positive function, every dip pole is a minimum for H.

Since $\cot I=H/Z_o$ where Z_o is the value at the dip pole, the isoclines form a similar family of ellipses as in (5) except for a difference in parameters. The gradient is given by

$$\frac{\partial I}{\partial\rho}=\frac{(-\sin^2 I)}{Z_o}(a^2\cos^2\beta+b^2\sin^2\beta)^{\frac{1}{2}} \tag{6}$$

Since the dip pole is either a principal maximum or minimum with values of $\pm 90°$, the function I also has no unique gradient at the pole and as such is also not regular. However, since Z_o is quite large and dominates (6), the gradient is not as steep as in the previous case and is therefore easily amenable to normal smoothing techniques. The angular member that does pose difficulties is the magnetic declination D.

As is well known (CHAPMAN, 1941), the isogonic lines have a ray pole characteristic at both the geographic pole and the dip pole. Even though in the former case it is a uniform ray pole, it is still not very amenable to smoothing techniques.

In the case of the geographic pole, the convergence of D is due to the geometry of the system, it is the pole of the axis or the origin of the coordinate

system. The use of grivitation (subtraction of the east longitude at the point from the value of the declination there, this is only meaningful on a polar stereographic projection) will result in the removal of the singularity there. However, we still need a pair of functions that contain the same geomagnetic information as D and H but are free from singularities at the dip pole.

The following method was devised by KNAPP (1966) for finding a set of substitution functions for D and H. A polar stereographic projection centered on the geographic pole is used as is the mild requirement that the pattern representing the isolines in the neighborhood of a dip pole shall have zero curl (the field has a scalar potential). Since we only are concerned with focal dip poles (this is in contrast to dip poles whose contour lines form parabolas or hyperbolas and are referred to as nodal and cuspidal and are not likely in the area being discussed; see CHAPMAN, 1940 and 1941), the curves of equipotential will be closed curves encompassing the dip pole similar to eq (4). Then resolving the horizontal component of the field into two orthogonal components P and Q that are respectively in directions x and y of the previously mentioned rectangular grid for eq (4) we obtain

$$\begin{aligned} P &= H\cos(D-L_d) \\ &= X\cos L_d + Y\sin L_d \\ Q &= H\sin(D-L_d) \\ &= Y\cos L_d - X\sin L_d \end{aligned} \tag{7}$$

where X and Y are the usual north and east components and L_d is the longitude reckoned from a reference meridian L'; 83°W for the Arctic and 77°W for the Antarctic, so that $L_d = L' + L_g$ where L_g is the East longitude from Greenwich. This choice of reference meridians allows the previously mentioned grid to conform to the axis of the elongation and guarantees that the P and Q isolines will be perpendicular and relatively straight in a fairly large area around the dip pole, thereby simplifying the smoothing procedure.

The advantage obtained from the use of these two substitution functions is their continuity over the singular points of D and H. The focal dip pole can be easily located by the intersection of the P and Q zero isolines. Once P and Q are determined, D and H can be recovered from

$$\begin{aligned} D &= L_d + \arctan Q/P \\ H &= (P^2+Q^2)^{\frac{1}{2}} \end{aligned} \tag{8}$$

Comparison of the Model Fields in Antarctica

The various fields produced by the models were compared on a 5° by 10° grid in latitude and longitude south of the 40°S parallel. Table 1 indicates the rms differences between the N&O and CAIN models for 1960 and for the LME and HKNW models for 1965. It should be noted that the N&O coefficients had to be updated to 1960 which may in part account for the greater variation.

Table 1. RMS differences and south dip pole locations. The root-mean-square difference values for the 1960 and 1965 models are given along with the locations of the south dip pole given by the models.

Model	Dates	South dip pole location		RMS differences between pairs of models		
				D	*I*	*H*
N&O	1960			3.0°	0.93°	774 gammas
CAIN	1960					
LME	1965	66.5°S	140.0°E	0.76°	0.43°	185 gammas
HKNW	1965	66.5°S	139.0°E			

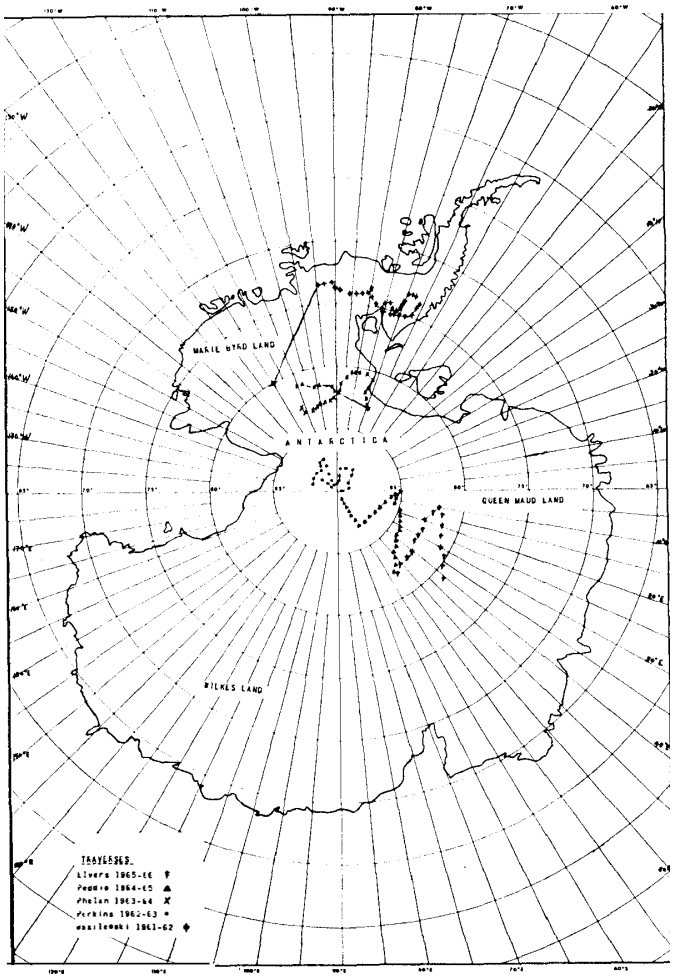

Fig. 2. Antarctica chart giving the location of the traverses and various observation points.

Antarctic Traverses

Five of the most recent traverses available were compared to the field values generated by the models along the traverse path; See Fig. 2 for the location of the traverse routes. The traverses used in the comparison to the 1965 LME and HKNW models were the 1965–66 traverse of ELVERS (1966), the 1964–65 traverse of PEDDIE (Internal C&GS publication), and the 1963–64 traverse of PHELAN (1965). The traverses compared to the N&O and CAIN 1960 models were the

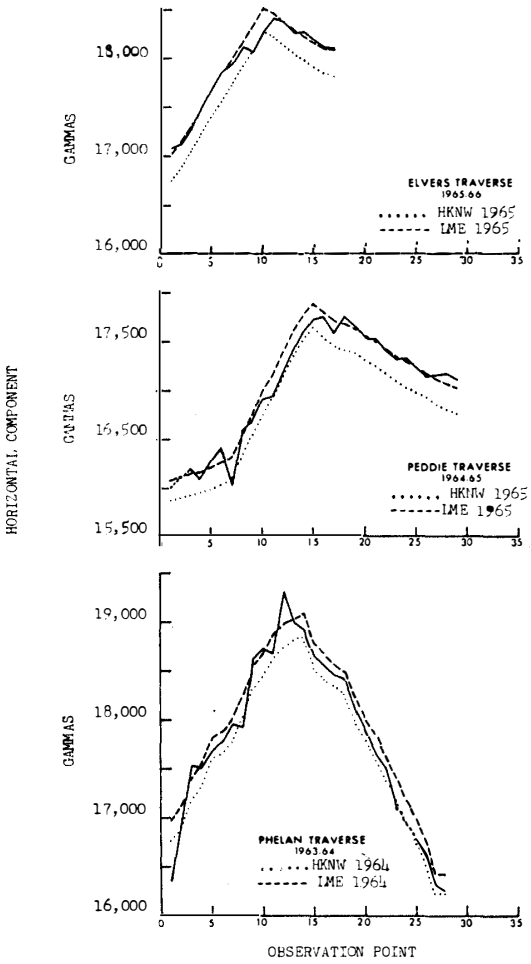

Fig. 3. Horizontal component comparison between traverses and the 1965 models updated to the dates of the traverses. The abscissa gives the observational point number, the distance varying between any two points.

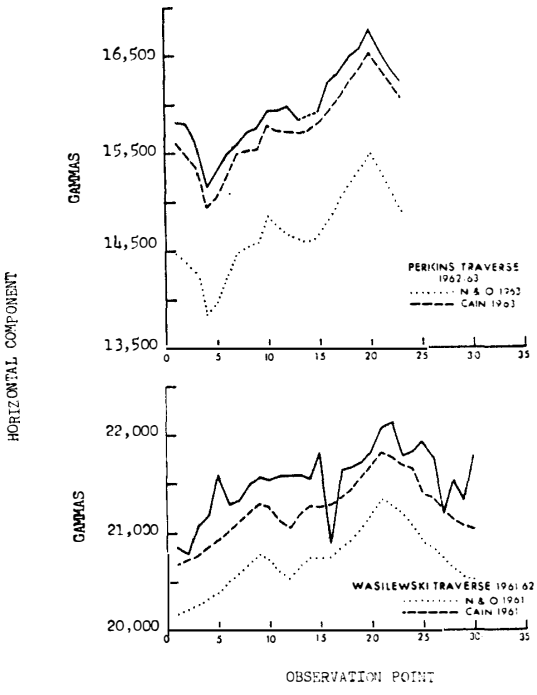

Fig. 4. Horizontal component comparisons between the traverses and the 1960 models updated to the dates of the traverses. The abscissa gives the observational point number, the distance varying between any two observation points.

1962–63 traverse of PERKINS (1964) and the 1961–62 traverse of WASILEWSKI (Internal C&GS publicatation). With the exception of the HKNW model, the secular change coefficients were used to update the models to the dates of the traverses. As of yet there are no HKNW secular change coefficients available so the LME values of secular change were used for both of the 1965 models instead. In comparing the observed and computed values, a converted random point synthesis program written by Mr. L. HURWITZ of the USC&GS was used to compute the field at every point where observations were taken.

Table 2 gives the RMS and greatest deviation values for the various models and traverses for *I* and *D*. For the 1965 models, the LME values generally approximated the observed values more accurately; the HKNW values were usually greater in absolute value than either the LME or traverse values. There is one obviously bad point on the PHELAN traverse where the deviation in *D* is over 10° with both models agreeing within 0.002°.

The comparison for the 1960 N&O and CAIN models is not as favorable. The CAIN values tend to give a closer approximation than those of the N&O model.

Referring to Figs. 3 and 4, we have the comparison of the model and traverse values for the *H* component. The abscissa has the traverse number of the observations. The distance between any two points of observation varied from traverse to traverse and from point to point.

The observed values were bracketed by the values for the LME and HKNW models with the LME values being the greater. The comparison is not so favorable for the N&O and CAIN models. The observed values are consistently

Table 2. RMS and maximum deviation of I and D between traverse and model values. The root-mean-square and maximum deviations from the traverse observations are given for each of the models for the I and D magnetic elements. The asterisk (*) indicates the values with (top) and without the inclusion of the "bad" value mentioned in the text.

Traverse	Model	RMS *I*	MAX DEV *I*	RMS *D*	MAX DEV *D*
ELVERS	LME	0.17°	0.27°	1.33°	1.69°
	HKNW	0.65°	1.56°	1.87°	2.51°
PEDDIE	LME	0.14°	0.28°	1.38°	3.22°
	HKNW	0.49°	1.25°	1.67°	2.28°
PHELAN	LME	0.24°	0.67°	*2.33° 0.79°	*10.32° 0.76°
	HKNW	0.21°	0.71°	*2.36° 0.81°	*10.32° 0.83°
PERKINS	CAIN	0.28°	0.34°	0.35°	0.94°
	N&O	1.46°	1.66°	4.56°	4.53°
WASILEWSKI	CAIN	0.68°	2.96°	0.55°	1.81°
	N&O	0.93°	3.53°	3.21°	3.72°

greater than either model but the variation is much greater than in the previous case. Both models have the same general profile as the observed field but the CAIN values are closer to the observed field than are the N&O values by about 500 gammas for the WASILEWSKI traverse and by about 1100 gammas for the PERKINS traverse.

Conclusions

The higher the degree and order of the analysis, the better the approximation should be to the observed field. This is, of course, obvious, the field being exactly represented if the analysis could be carried out to high enough order and degree. It has been suggested that no more than $m=n=10$ is necessary to approximate the field within the limits acceptable for world charts (ALLDREDGE *et al.*, 1963).

It would appear that we have a contradiction to the above statement in that the LME ($n=m=8$) analysis compares more favorably with recent traverse data in the region under investigation than does the HKNW ($n=m=12$) analysis. However, the method of data manipulation and smoothing must be considered. For second and subsequent analyses, the LME method superimposed observed values on the working charts where it was believed that the addition of these non-grid values was more accurate than the interim analytic model. In general, the charts were being continually altered and the model (the coefficients) adjusted to conform to the known point value which were heavily weighted in the procedure.

This is in contrast to the HKNW analysis which used a more analytical approach throughout. All data were equally weighted and at points of singularity the method of KNAPP described previously was employed instead of the introduction and weighting of non-grid values. Also, the analytical presmoothing method of HKNW, described previously, avoided the subjective decisions of manual cartography of the LME method. The HKNW method lends itself particularly well to more efficient computer analysis which will become more valuable when the data explosion due to satellite surveys makes itself felt.

Manual smoothing and manipulation of the LME method gave better results in the Antarctic region than did the HKNW method which sacrificed some accuracy for a more analytical method and speed. However, in the future with the increased data, the LME method might become too cumbersome while the HKNW method would probably be preferred.

For the 1960 models, the CAIN analysis seems to be the more precise. It was indicated by NAGATA and OGUTI that their analysis was just a temporary one to be used until a more thorough analysis was completed. The CAIN model which was done later had the advantage of more and better data and was carried out to higher degree and order than the N&O analysis. Part of the variation may be due to faulty secular change since the N&O coefficients had to be updated originally to 1960 from 1958.5.

References

ALLDREDGE, L. R., G. D. VAN VOORHIS and T. M. DAVIS: A magnetic profile around the world. J. Geophys. Res., **68**, 3679, 1963.

CAIN, J. C.: Models of the earth's magnetic field. NASA Pub. X-612-65-400, 1965.

CAIN, J. C., W. E. DANIELS, S. J. HENDRICKS and D. C. JENSEN: An evaluation of the main geomagnetic field, 1940-1962. J. Geophys Res., **70** (15), 3647, 1965.

CHAPMAN, S.: Notes on isomagnetic charts I and II. J. Geophys. Res., **45**, 433 and 443, 1940.

CHAPMAN, S.: Notes on isomagnetic charts III and IV. J. Geophys. Res., **46**, 7 and 15, 1941.

CHAPMAN, S.: Solar Plasma, Geomagnetism and Aurora, Gorden & Breach, New York, P1-5, 1964.

CHAPMAN, S., and J. BARTELS: Geomagnetism, Oxford Press, London, 2v, 1940.

ELVERS, D.: Results of the 1965-66 Antarctic traverse, in preparation at the USC&GS, 1966.

FLEMING, J. A.: Terrestrial Magnetism and Electricity, Physics of the Earth VIII, McGraw-Hill, New York, Ch 1, 1939.

HURWITZ, L., D. G. KNAPP, J. H. NELSON, and D. E. WATSON: Mathematical model of the geomagnetic field for 1965. J. Geophys. Res., **71** (9), 2373, 1966.

KNAPP, D. G.: Charting magnetic dipoles and associated patterns, 1966 (in press).

LEATON, B. R.: Improving world magnetic charts. MNRAS, Geophys. Suppl., **7**, 319, 1957.

LEATON, B. R., S. R. C. MALIN, and M. J. EVANS: An analytical representation of the estimated geomagnetic field and its secular change for epoch 1965.0. J. Geomag. Geoelec., **17** (4-4), 187, 1965.

NAGATA, T. and T. OGUTI: Magnetic charts for the epoch of 1958.5 corrected for the Antarctic region and spherical harmonic coefficients of the revised geomagnetic field. J. Geomag. Geoelec., **14** (2), 125, 1962.

NELSON, J. H., L. HURWITZ and D. G. KNAPP: Magnetism of the earth. Dept. of Commerce Pub. 40-1, 1962.

PERKINS, D. M.: Magnetic results South Pole traverse 1962-63, USC&GS 1964.

PHELAN, M.: Magnetic results Filchner Ice Shelf traverse 1963-64, USC&GS 1965.